

MRI for Dental Applications



Husniye Demirturk Kocasarac, DDS, PhD^{a,*}, Hassem Geha, DDS, MDS^a,
Laurence R. Gaalaas, DDS, MS^b, Donald R. Nixdorf, DDS, MS^c

KEYWORDS

• MRI • Dental MRI • UTE • SWIFT • ZTE • FLASH • Tooth • Jaw

KEY POINTS

- MRI is a well-developed medical imaging technology, being the imaging modality of choice for most soft tissue and functional imaging indications.
- The science and application of MRI continue to advance, with several recent developments having notable implications for the practice of dentistry.
- Although MRI has traditionally been considered prohibitively costly for use in routine dental practice, many of the recent technological advancements have the potential to greatly reduce the cost associated with manufacturing and operating an MRI scanner.

INTRODUCTION

Visualize an MRI scanner that is less expensive and designed to image a smaller field of view (FOV), like a knee, ankle, or wrist. Such anatomy-specific MRI scanners have been developed and are currently or soon to be available.¹ Facilitating this development is an MRI design shift away from using larger and more expensive magnets with excellent field homogeneity and toward accepting smaller, less homogeneous (or less perfect) magnetic fields produced by cheaper and smaller magnets. Image formation can remain feasible by computationally correcting for magnet inhomogeneity and technological advances in pulse sequences and coil design, allowing for MRI scanners to become even cheaper to manufacture.^{1–3} Now, imagine optimizing these smaller FOV scanners to image teeth, the jaws, and face, and you have the design of an MRI scanner designed for dental use.

The physics of producing an image with magnetic resonance are more complex and quite different from computed tomography (CT) or cone beam computed tomography

Disclosure: The authors have nothing to disclose.

^a Division of Oral and Maxillofacial Radiology, Department of Comprehensive Dentistry, University of Texas Health San Antonio, 7703 Floyd Curl Drive, San Antonio, TX 78229, USA;

^b Oral and Maxillofacial Radiology, Division of Oral Medicine, Diagnosis and Radiology, Department of Diagnostic and Biological Sciences, School of Dentistry, University of Minnesota, 7-536 Moos Tower, 515 Delaware Street Southeast, Minneapolis, MN 55455, USA; ^c Division of TMD and Orofacial Pain, Department of Diagnostic and Biological Sciences, School of Dentistry, University of Minnesota, 6-320 Moos Tower, 515 Delaware Street SE, Minneapolis, MN 55455, USA

* Corresponding author.

E-mail address: demirturk@uthscsa.edu

Dent Clin N Am 62 (2018) 467–480

<https://doi.org/10.1016/j.cden.2018.03.006>

0011-8532/18/© 2018 Elsevier Inc. All rights reserved.

dental.theclinics.com

(CBCT) using radiograph. Consequently, MRI has considerably more opportunity for producing useful depictions of human tissues. With the development of dental and face-specific MRI coils, plus the freedom found in sequence design and image processing, researchers can feasibly develop custom techniques to address any number of dental imaging indications: anatomic characterization of hard tissues including bone and teeth for “routine” dental indications like implant placement, caries detection, and fracture detection; anatomic and functional characterization of soft tissues, including periodontal/periapical inflammation, muscle and nerves to characterize neural and pain disorders, and pathologic tissue characterization to diagnose neoplasms and dysplasia without a surgical biopsy; blood flow imaging in both bulk and perfusion forms to assess tissue viability/inflammatory status; and finally, spectroscopy to provide molecular profiles of tissue. Related technological advances in pulse sequence design will likely lead us into uncharted knowledge about normal dental anatomy and physiology as well as pathology and pathophysiology.

In this article, the authors provide a brief overview of the use of conventional MRI techniques applied to dental indications, discuss relevant MRI physics in the various steps of image formation, and highlight recent hardware and software technical developments that contribute to (1) the cost/size of MRI decreasing significantly, allowing use in the typical dental clinic, and (2) the facilitation of very specific dental imaging applications that will solve clinical problems.

ESTABLISHED MRI TECHNIQUES APPLIED TO DENTAL INDICATIONS

The first MRI was acquired by Lauterbur in 1973.⁴ With the evolution of the commercial medical MRI in the 1980s, several applications were performed in medical imaging (ie, cardiac, abdominal, cranial MRI).⁵ Broadly, in medicine, MRI is fast outpacing any other modality for in vivo displaying of soft tissues and function in the human body without any invasive procedure and ionizing radiation.⁶ Because of the inability of conventional MRI to image hard tissues, conventional MRI techniques in dentistry have been mostly used for soft tissue imaging, including the temporomandibular joints (TMJ), soft tissues, tumors, salivary glands, and maxillary sinuses.⁷ Currently, TMJ imaging comprises the vast majority of dedicated MRI imaging for clinical dental indications with diagnostic accuracy of joint characterization and disc localization high enough that the modality is considered the gold standard.⁸⁻¹⁰

Other applications of MRI for dental indications include caries detection, pulpal/periapical disease characterization, and some efforts at inferior alveolar nerve identification. These efforts have been limited largely to research/experimental reports and have not been adopted clinically. The use of MRI to visualize dental caries was first described by van Luijk in 1981¹¹ with later studies stating that the caries under a restoration, which cannot be easily seen on a conventional radiograph, may be detected by MRI in the future.⁵

MRI for pulpal and periapical disease characterization appears promising with successful imaging of pulp morphology, visualization of pulpitis/pulp vitality, and assessment of pulpal regeneration.¹² MRI has demonstrated some experimental utility in identifying the location of the mandibular nerve in the context of mandibular dental implant and surgery planning.^{13,14}

A BRIEF OVERVIEW OF MRI PHYSICS AND STEPWISE DESCRIPTION OF HOW AN MRI IS OBTAINED

Before recent developments in MRI research specific to dental imaging and as a matter of review are discussed, the following is a brief discussion of how diagnostic images are obtained using MRI.

Step 1. Place a Patient in a Large Magnet

Every single hydrogen (hydrogen-1) nucleus in a patient or object otherwise has its own tiny magnetic field. Hydrogen nuclei (mostly water) in aggregate have essentially randomly oriented magnetic fields, but when placed in a strong magnetic field, they align and incur precession (resonance) with the magnetic field like tiny spinning tops. Accordingly, when a patient or object is placed in an MRI magnetic field, every hydrogen nucleus aligns and incurs precession in the direction of the magnetic field, the first step in enabling capture of a MR image. Generally, MRI units are measured by the strength of the magnet with units of Tesla, where 1 T is the equivalent of 20,000 times the magnetic field strength of Earth. The vast majority of clinical MRI scanners in use today are either 1.5 T or 3 T for human procedures.⁶

Step 2. Use a Transmitting Radiofrequency Coil to Apply a Radiofrequency Pulse to the Patient in the Magnet

With the application of a radiofrequency (RF) pulse to the patient in the magnet, all of the patient's hydrogen nuclei realign their direction of precession to the direction of a RF pulse. Transmitting RF coils are typically built into the larger body of the physical MRI unit, with the magnet. The RF pulse is left on for variable amounts of time to initiate different degrees of resonance or realignment with the RF pulse. During realignment, all of the hydrogen nuclei absorb some amount of energy and create a new, tiny magnetic field in alignment with the applied RF pulse. This degree of energy input can be deliberately applied in order to emphasize or deemphasize various tissue types that otherwise can overall overwhelm aspects of an MRI image. Fat-suppressed images are one common example of this technique, in which the proper amount of RF energy applied later on results in minimal or zero contribution of fat to the image allowing better visualization of adjacent tissues of interest.^{15,16} Similarly, fluid attenuated inversion recovery eliminates high signals seen from fluid/water and is used to detect parenchymal edema without the glaringly high signal from cerebrospinal fluid.¹⁷⁻¹⁹

Step 3. Stop the Radiofrequency Pulse and Use a Receiving Radiofrequency Coil to Collect and Record Radiofrequency Energy Released by the Hydrogen Nuclei as They Realign Back to the Original Magnet Field of the MRI Unit

A receiving coil used to collect and record the RF energy released by the patient may be the same coil as the transmitting coil (typically built into the scanner body), or it could be a separate receiving-only coil designed for imaging specific anatomic regions. These coils are commonly called "surface" coils because they are separate from the larger MRI physical unit, and they are applied close to the surface of the patient's anatomy to be imaged.

When hydrogen nuclei "relax" back to precession in alignment with the primary magnetic field of the unit, they do so with primarily 2 characteristic properties: T1 and T2. T1, or spin-lattice relaxation time, refers to an average time a group of hydrogen nuclei relax back to their initial energy level before the RF pulse. T2, or spin-spin relaxation time, refers to an average time a group of hydrogen nuclei having been subject to an applied RF pulse loses the tiny magnetic field created in alignment with that RF pulse. In practice, T1 sequences are common images in any MRI evaluation and are usually used as "anatomic" images.^{20,21} Based on both the environment surrounding hydrogen nuclei (based largely on tissue type) and the overall concentration of hydrogen nuclei (also based largely on tissue type), different tissues have different T1 and T2 properties. The amount of T1 and T2 signal can be converted into pixel grayscale value once reconstructed. In pure T1-weighted images, fatty tissue demonstrates typically a high signal (bright), whereas muscles and other soft

tissues demonstrate intermediate signal intensity (gray), and fluid demonstrates a low signal (black).

As discussed earlier, a fat-suppressed T1-weighted image is a variation of a T1 sequence where the bright signal from fat is cleverly eliminated (suppressed) for detection of other tissue's signals that can be obstructed by the fat signal.^{15,16} In a contrast-enhanced T1-weighted image, a gadolinium-based contrast agent is injected intravenously, and scans are obtained a few minutes after administration. The gadolinium acts to shorten both T1 and T2 properties, thereby increasing tissue signal and ultimately image brightness. Because the contrast agent is applied intravenously, vascular structures and any pathologic condition with increased vascularity appear brighter on the MRI image. Frequently, postcontrast T1 sequences are also fat suppressed to make them easier to interpret.²² T2 sequences are also common images in any MRI evaluation and are usually used as simplified "functional" or "pathologic" images because in many pathologic conditions, the water content increases, leading to an increase in the signal of those pathologic tissues.^{20,21}

Proton density images represent an "overall" density of hydrogen in the patient with an image that is not biased or weighted to either T1 or T2 character. Proton density images are commonly used for brain imaging and also are excellent for TMJ imaging because they offer excellent signal distinction between fluid, hyaline cartilage, and fibrocartilage.^{23,24} Diffusion-weighted imaging assesses the ease with which water molecules move around within a tissue and give insights into cellularity, cell swelling, and edema.^{25,26}

Conventional MRI cannot easily show hard tissues, including bone and teeth, because of the low concentration of hydrogen protons that contribute to the magnetization, and also because of extremely fast T2 relaxation times not detectable with conventional techniques.²⁷ In other words, the signal from mineralized dental tissues decays faster than signal of liquids before MRI signal is detected. This phenomenon causes minimal or no image intensity (black image) MR images.²⁷

MRI has an obvious advantage in the lack of use of ionizing radiation and associated added risk of cancer development to the patient; however, it should be noted that the presence of a strong magnetic field can affect ferromagnetic metals in the vicinity of the magnet. Therefore, MRI is typically not used for patients with cardiac pacemakers, implantable defibrillators, artificial heart valves, cerebral aneurysm clips, or ferrous foreign bodies in the eye.⁸

Technical developments enabling dental-specific MRI

There are several required main components to successfully image a patient or object with MRI: a strong magnet, body or surface coils, gradient coils, a pulse sequence, and software for digitized image reconstruction/manipulation/display. The authors describe these components along with recent technical developments they think will enable the construction of less expensive and dental-specific MRI units.

THE MAGNET

The largest component of a typical MRI scanner is the magnet itself, which is in essence a large insulated vessel containing wire windings and cryogen (ie, liquid helium) to enable a superconducting magnet. The manufacturing process for magnets with a small bore size requires less wire and cryogen and is therefore smaller, lighter, and cheaper. These smaller magnets facilitate the development of scanners that are dedicated in their purpose, such as dedicated head, knee, wrist, breast, or small animal imaging. This transition of large, whole-body MRI scanners to smaller, dedicated-

purpose MRI scanners is similar to the development of a dental CBCT scanner from a multipurpose medical CT scanner.

Furthermore, the advent of high-temperature superconducting wire has eliminated the need for cryogenics, which is expensive to purchase and bulky to use because of the required insulation and the need to pressurize the container that houses the windings.²⁸ These magnets are “plug in the wall” powered, with the only remaining major barrier to development the cost of manufacturing high-temperature superconducting material in continuous lengths needed for MRI use. An alternative approach to avoiding the use of cryogenics is to use rare earth magnets, which have all the same benefits as high-temperature superconducting wiring but also have a high cost.²⁹ Rare earth magnets are also disadvantaged by their inability to achieve strong magnetic fields, such as 1.5 T, a minimum standard for obtaining high-quality images. The combinations of anatomy-specific scanners and scanners that avoid the use of cryogenics result in systems greatly reduced in size, weight, and complexity, all requirements needed to realize the development of point-of-care dental MRI scanners. The potential development of a commercial market plus mass production of high-temperature superconducting wire will allow for a reduction in cost of manufacturing, further reducing overall costs.

BODY AND SURFACE COILS

Clinical MRI scanners are built with large RF coils within the bore of the scanner to transmit radio waves that energize the tissue being imaged. These RF coils are typically referred to as body coils, because they are built to energize the entire body, regardless of the anatomy being imaged. To record the RF signal released by the patient, anatomy-specific receiver or surface coils are placed adjacent to the anatomy being imaged. Per the discussion earlier, MRI scanners that are anatomy specific, such as a head-only scanner, reduce the need for these large body coils and associated cost. An alternative approach is to use transceiver coils that both transmit and receive the RF signal, thus eliminating the need for body coils altogether.³ Because a coil acts as an antenna by detecting the signal emitted from the patient, the closer distance the coil is to the anatomy of interest to be imaged results in a greater amount of detectable signal from the tissue of interest. Consequently, designing coils to be anatomy specific allows for a smaller FOV to be used, and it results in the ability to decrease the voxel dimensions, thus increasing the capacity to obtain higher resolution images (Figs. 1 and 2).³⁰ The acquisition of high-resolution images is critical for dentistry, because visualization of small alterations in anatomy is commonly clinically significant. This approach has been used for dental applications, such as the extraoral approach of obtaining a close fit of the coil over the face,^{31,32} and the intraoral approaches of placing the coil adjacent to the teeth (like a periapical film)³⁰ or in the orthogonal plane (like an occlusal film).³³ To improve comfort and usability, coils that transmit signal to the scanner wirelessly have been developed (Figs. 3 and 4).³⁴ It is hoped that the development of coils specific to teeth and supporting structures will enable FOVs that image not only teeth effectively but also the surrounding periodontium and alveolar bone.³³

GRADIENT COILS

Gradient coils are located in the body of the magnet proper. The function of these coils is to impart a small change or gradient within the main magnetic field in each of the 3 dimensions of the patient, referred to as x-, y-, and z-directions. While the magnet is scanning, these gradient coils will be used to rapidly alter the local magnetic field, with

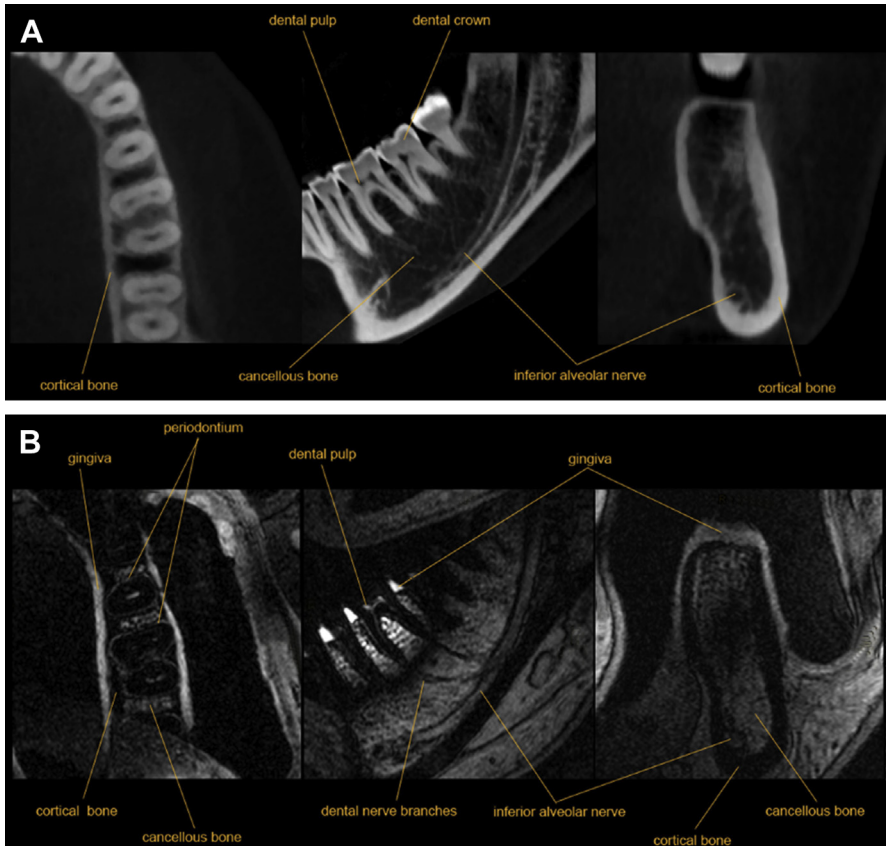


Fig. 1. (B) Axial (left), sagittal (middle), and transverse (right) cross-sections of FLASH MRI of the lower jaw acquired in vivo with an intraoral coil that was inductively coupled to a small loop coil at 3 T with the following parameters: $250 \mu\text{m}^2 \times 500 \mu\text{m}$ resolution, $64 \text{ mm} \times 64 \text{ mm} \times 28 \text{ mm}$ FOV, acquisition time 3:57 minutes. (A) Axial (left), sagittal (middle), and transverse (right) cross-sections of in vivo cone beam CT of the lower jaw (3D Accuitomo 170, Morita, Japan; nominal resolution, $250 \mu\text{m}$, 90 kV, 201 images). (From Flügge T, Hövener JB, Ludwig U, et al. Magnetic resonance imaging of intraoral hard and soft tissues using an intraoral coil and FLASH sequences. *Eur Radiol* 2016;26:4621; with permission.)

larger gradients producing a greater ability to record spatial information. The rapid changes in gradients are responsible for producing the noise associated with MRI scanning, with some pulse sequences demanding fast and large gradient changes and associated noise (eg, functional MRI). A notable advantage of sweep imaging with Fourier transformation (SWIFT), a relatively new pulse sequence that has shown success at imaging hard tissue of teeth and bones, is relatively little demand on gradient coil changes and associated low noise/improved comfort for the patient.²⁷

PULSE SEQUENCES

A pulse sequence is the code that instructs the MRI scanner in how to image the patient, similar to how software instructs a computer how to operate. Over time, new pulse sequences are developed to address new approaches to imaging, and clinically

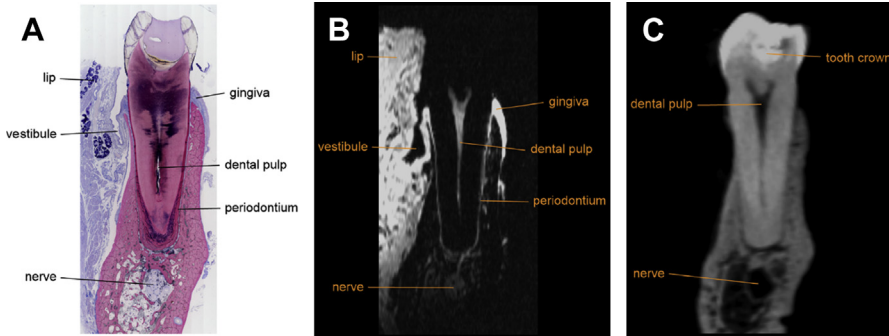


Fig. 2. (A) Histologic section through the second premolar in the left mandible of an ex vivo human specimen. (B) Section through the MRI of the tooth with identical visible structures. (C) Section through CBCT image of the ex vivo human specimen with fewer visible structures. (From Flüggé T, Hövener JB, Ludwig U, et al. Magnetic resonance imaging of intraoral hard and soft tissues using an intraoral coil and FLASH sequences. *Eur Radiol* 2016;26:4619; with permission.)

robust ones are continuously updated. Also similar to computer software, matching the software (ie, pulse sequence) and the hardware (ie, magnet and coil) with each other is critical to get maximal production and efficiency for a given MRI scanner. The pulse sequence developments that are allowing the visualization of densely calcified tissue (eg, dentin, enamel, bone) are referred to as short T2, because they allow for capture of the rapidly decaying T2 signal inherent to hard tissues. SWIFT, ultrashort echo time (UTE), and zero echo time (ZTE) are all examples of relatively newly developed short T2 pulse sequences with efficacy in imaging hard tissue.

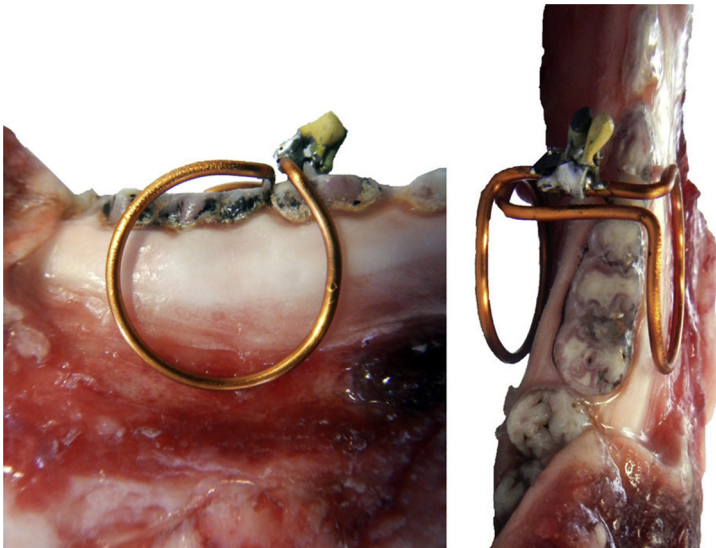


Fig. 3. Typical placement of an intraoral coil (here: C2) on a porcine mandible for ex vivo MRI. (From Ludwig U, Eisenbeiss A-K, Scheifele C, et al. Dental MRI using wireless intraoral coils. *Sci Rep* 2016;6:23301. This work is licensed under a Creative Commons Attribution 4.0 International License, Available at: <http://creativecommons.org/licenses/by/4.0/>.)

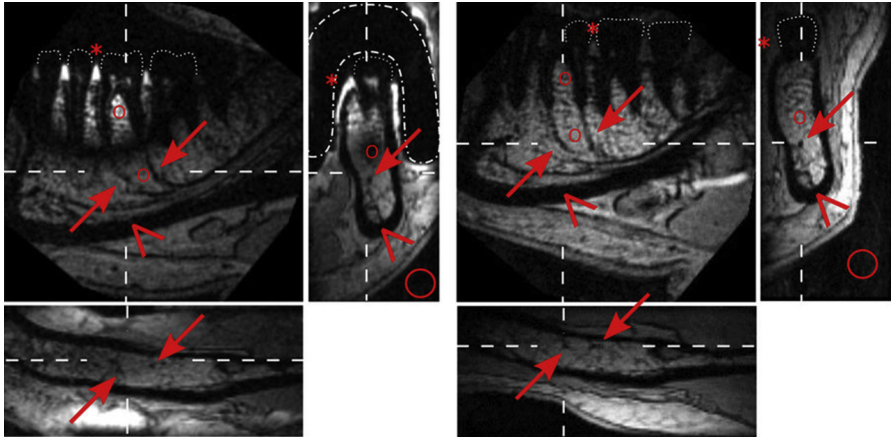


Fig. 4. In vivo dental MRI of a mandible acquired with (*Left*) and without (*Right*) intraoral coil C3 in conjunction with a 4-cm loop coil. Orthogonal slices were reconstructed from a 3D-FLASH MRI that was acquired in 3:57 minutes at 3 T at a resolution of $250 \mu\text{m}^3 \times 250 \mu\text{m}^3 \times 500 \mu\text{m}^3$. Note that the intraoral coil enhanced the signal of the inter-dental gingiva (*asterisk*) and pulp strongly and caused a signal hypointensity at the roots. Both configurations nicely depicted the inferior alveolar nerve and its branches to the apices of the teeth (*rami dentales*) as indicated by arrows and wedges, respectively. Dashed lines indicate the position of the reconstructed slices; dotted lines indicate the crowns of the teeth, and dash-dot lines indicate the position of the intraoral coil. The regions where the signal and noise was measured are indicated by asterisks (*gingiva*) and circless. (*From* Ludwig U, Eisenbeiss A-K, Scheifele C, et al. Dental MRI using wireless intraoral coils. *Sci Rep* 2016;6:23301. This work is licensed under a Creative Commons Attribution 4.0 International License, Available at: [http://creativecommons.org/licenses/by/4.0/.](http://creativecommons.org/licenses/by/4.0/))

In one of the first clinical studies assessing the feasibility of UTE sequence, it was reported that UTE sequence could identify caries lesions at an earlier stage than conventional radiograph techniques, but it required 25 minutes for the imaging of a single tooth (**Fig. 5**).³⁵ This finding can be explained by the substantial mineral breakdown required for radiograph display, which is preceded by local acid formation that is likely to be detected with MRI.³⁶

The feasibility of the ZTE sequence to assess tooth tissue components has been investigated in vitro. ZTE sequence, applied to extracted human teeth at 11.7 T, yielded very good depiction of the mineralized dentine and enamel layers. In addition, compared with micro-CT, ZTE MRI was found to be less sensitive to artifacts resulted from dental restorations and to have superior sensitivity for the detection of early demineralization and caries lesions (**Fig. 6**).³⁶

SWIFT sequence, with a short TE using intraoral coil, enabled simultaneous imaging of both soft and hard dental tissues with a high resolution and in a relatively short scanning time (10 minutes). Despite soft tissues not being displayed in detail, this technique appears to be promising and practical for clinical applications. The sequence also showed promise in determining the extent of carious lesions and the status of pulpal tissue, whether reversible or irreversible pulpitis.²⁷

In a recent study performed by using SWIFT sequence, with a cable-bound intraoral coil, teeth of the upper and lower jaw were displayed in vivo in 4.5 minutes. It was also stated that the first MRI panoramic images at such high nominal resolution (0.3 mm^3)

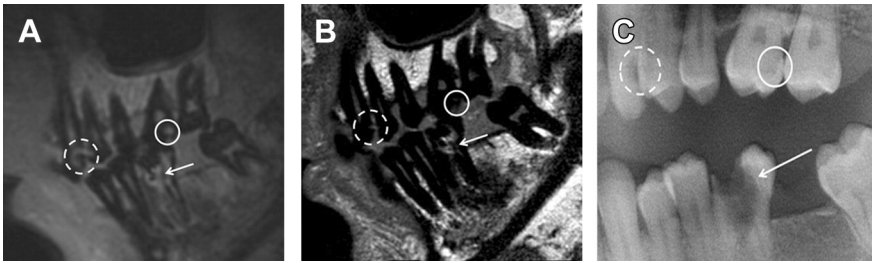


Fig. 5. Appearance of an initial caries (CIII, circle), secondary caries in the proximity of an amalgam filling (CI, dashed circle), and progressed caries lesion with related breakdown of the enamel and dentin layer (CI, arrow) in UTE (A), spin echo (B), and XR (C). (From Bracher AK, Hofmann C, Bornstedt A, et al. Feasibility of ultra-short echo time (UTE) magnetic resonance imaging for identification of carious lesions. *Magn Reson Med* 2011;66(2):542; with permission.)

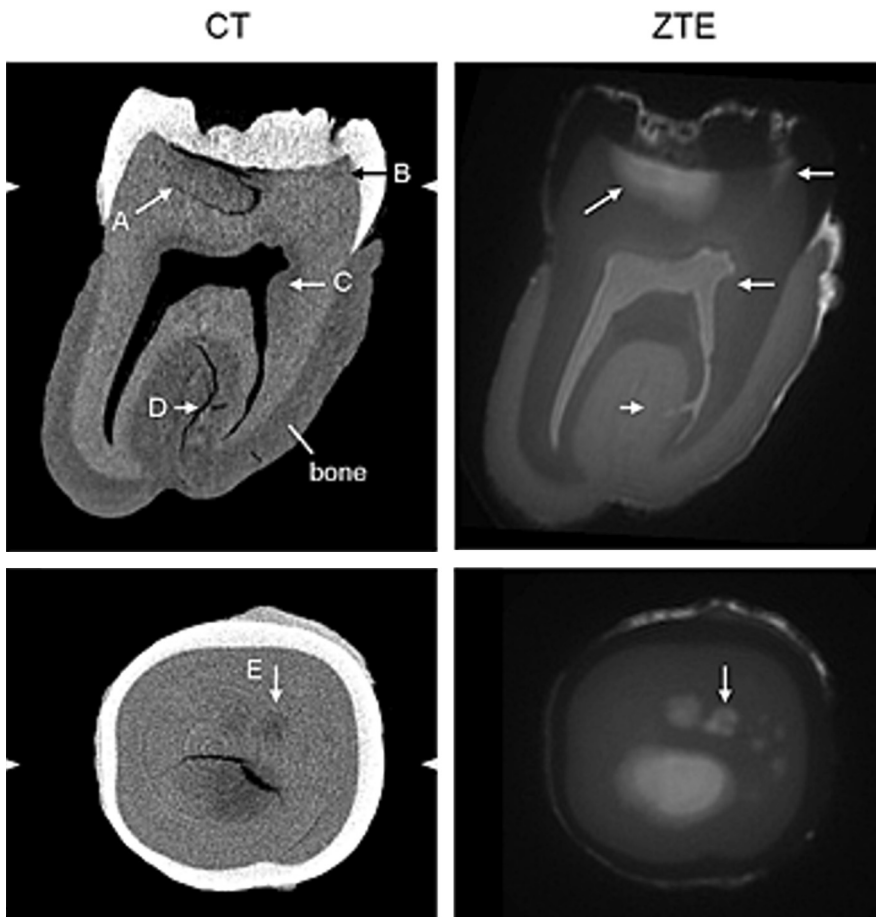


Fig. 6. μ CT and ZTE MR images acquired from a molar with caries lesions. Some residual bone attached to the teeth is visible. Occlusal demineralized lesion (arrows A,B), Halo effect around the pulp (arrow C), the fissures visible with μ CT inside the dentine (arrow D), demineralized lesions (arrow E). (From Weiger M, Pruessmann KP, Bracher AK, et al. High-resolution ZTE imaging of human teeth. *NMR Biomed* 2012;25(10):1148; with permission.)

were achieved. With this approach, the periapical region, alveolar bone, and inferior alveolar nerve were not visualized (**Fig. 7**).³³

One interesting attribute of the use of T2-weighted images is improved visualization of water content in hard and soft tissue. One study demonstrated the use T2 sequences in identifying cracks in teeth, specifically the contrast between relatively water-poor dental hard tissue and the small abnormality of a crack that contains more water content. As verified by micro-CT, fractures smaller than the voxel size of the MRI scan were visualized simply because of overwhelming signal from water content in the crack.³⁷

More excitingly, 4D imaging can be used to measure blood flow in tissue. This technique is established in medicine for assessing perfusion in brains injured from a stroke.³⁸ Translating this approach to dental applications, emerging data suggest that blood flow in teeth can be measured, a development that may mark drastically improved assessment of tooth pulp vitality and disease status (**Fig. 8**). Other indications may include tracking and recording real-time TMJ/mandibular movements. MR spectroscopy, another established technique in medicine,³⁹ may enable molecular characterization of various dental pathologic conditions, including inflammatory lesions, dysplasia, neoplasms, as well as characterization of normal tissue function. Diffusion tensor imaging, a relatively new variation of diffusion-weighted imaging, and other related sequences may represent an avenue of future mandibular nerve anatomic and functional imaging.^{40,41}

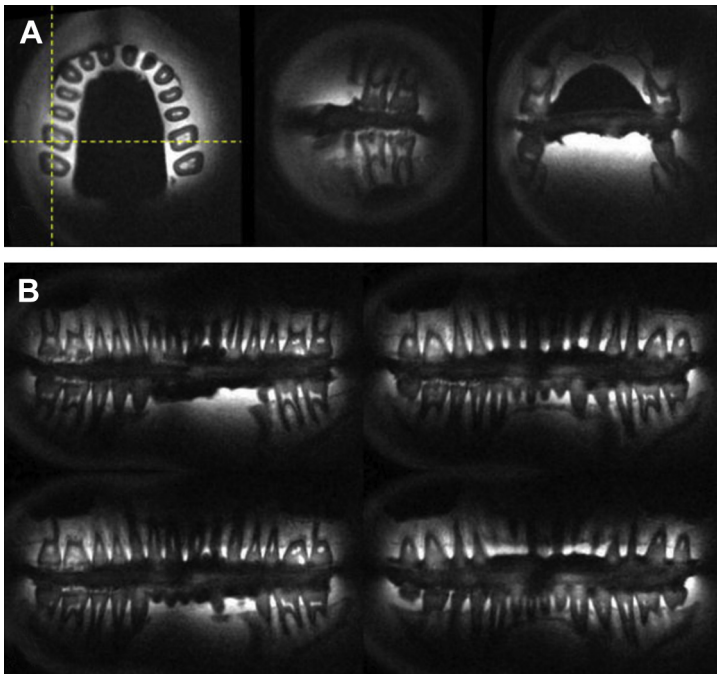


Fig. 7. Three selected orthogonal slices (A) and selected panoramic slices (B) of a 3D SWIFT image obtained using the transverse components of the B1 field. (From Idiyatullin D, Corum CA, Nixdorf DR, et al. Intraoral approach for imaging teeth using the transverse B1 field components of an occlusally oriented loop coil. *Magn Reson Med* 2014;72(1):164; with permission.)

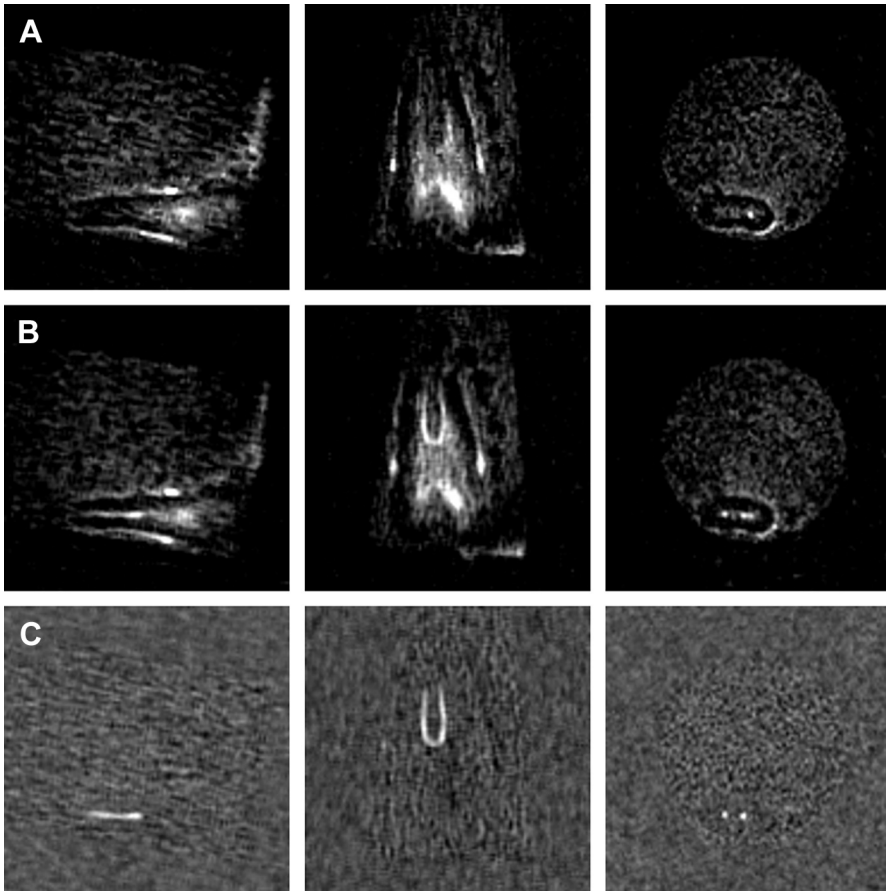


Fig. 8. (A) SWIFT MRI with blood-inflow saturation technique orthogonal sections of an extracted tooth with simulated fluid flow in the pulp chamber at 0.75 cm/s. (B) Similar orthogonal images with flow adjusted to 12 cm/s. (C) Image subtraction of 12 cm/s flow versus no flow demonstrating visualization of active fluid flow. These images are taken from unpublished data, 2017 performed by authors Nixdorf DR and Gaalaas L.

COMPUTING POWER AND IMAGE RECONSTRUCTION

In recent years, the computing power of personal computers built and priced for the consumer market have become adequate in handling most of the image reconstruction needs, thus decreasing the cost of MRI scanning systems. Only a few years ago MRI systems required expensive and purpose-built computer hardware to take the raw signals from the scanner and construct images from them. In addition, the algorithms for image reconstruction have improved, resulting in drastic reductions in time required to obtain useable images.

SUMMARY

In the last several years, major technological advancements involving multiple components of MRI have occurred. Together, they are enabling the hardware of MRI to become smaller, less complicated, cheaper, and tailored to acquiring images of teeth

and supporting structures. Research investigating the clinical utility of this technology to address problems in dentistry is just now initiating, and consequently, the application of MRI in dentistry is feasible with potential yet to be explored.

REFERENCES

1. Sutter R, Tresch F, Buck FM, et al. Is dedicated extremity 1.5-T MRI equivalent to standard large-bore 1.5-T MRI for foot and knee examinations? *AJR Am J Roentgenol* 2014;203(6):1293–302.
2. Snyder AL, Corum CA, Moeller S, et al. MRI by steering resonance through space. *Magn Reson Med* 2014;72(1):49–58.
3. Sohn SM, Vaughan JT, Lagore RL, et al. In vivo MR imaging with simultaneous RF transmission and reception. *Magn Reson Med* 2016;76(6):1932–8.
4. Scherzinger AL, Hendee WR. Basic principles of magnetic resonance imaging—an update. *The Western journal of medicine* 1985;143(6):782–92.
5. Tymofiyeva O, Boldt J, Rottner K, et al. High-resolution 3D magnetic resonance imaging and quantification of carious lesions and dental pulp in vivo. *MAGMA* 2009;22(6):365–74.
6. Shah N, Bansal N, Logani A. Recent advances in imaging technologies in dentistry. *World J Radiol* 2014;6(10):794–807.
7. Tymofiyeva O, Rottner K, Jakob PM, et al. Three-dimensional localization of impacted teeth using magnetic resonance imaging. *Clin Oral Investig* 2010;14(2):169–76.
8. Niraj LK, Patthi B, Singla A, et al. MRI in dentistry- a future towards radiation free imaging - systematic review. *J Clin Diagn Res* 2016;10(10):ZE14–9.
9. Suenaga S, Nagayama K, Nagasawa T, et al. The usefulness of diagnostic imaging for the assessment of pain symptoms in temporomandibular disorders. *Jpn Dent Sci Rev* 2016;52(4):93–106.
10. Boeddinghaus R, Whyte A. Trends in maxillofacial imaging. *Clin Radiol* 2018;73(1):4–18.
11. van Luijk JA. NMR: dental imaging without x-rays? *Oral Surg Oral Med Oral Pathol* 1981;52(3):321–4.
12. Arijji Y, Arijji E, Nakashima M, et al. Magnetic resonance imaging in endodontics: a literature review. *Oral Radiol* 2017. <https://doi.org/10.1007/s11282-017-0301-0>.
13. Chau A. Comparison between the use of magnetic resonance imaging and cone-beam computed tomography for mandibular nerve identification. *Clin Oral Implants Res* 2012;23(2):253–6.
14. Eggers G, Rieker M, Fiebach J, et al. Geometric accuracy of magnetic resonance imaging of the mandibular nerve. *Dentomaxillofac Radiol* 2005;34(5):285–91.
15. Bydder GM, Hajnal JV, Young IR. MRI: use of the inversion recovery pulse sequence. *Clin Radiol* 1998;53(3):159–76.
16. Lahrech H, Briguet A, Graveron-Demilly D, et al. Modified stimulated echo sequence for elimination of signals from stationary spins in MRI. *Magn Reson Med* 1987;5(2):196–200.
17. Lenclos N, Oppenheim C, Dormont D, et al. MRI of drug-resistant epilepsies: contribution of FLAIR sequence in a series of 150 patients. *J Neuroradiol* 2000;27(3):164–72 [in French].
18. Textor HJ, Flacke S, Pauleit D. Acute spinal epidural hematoma—comments on MRI diagnosis using fluid-attenuated inversion recovery sequence (FLAIR). *Rofo* 1999;170(2):231–2 [in German].

19. Morioka T, Nishio S, Mihara F, et al. Efficacy of the fluid attenuated inversion recovery (FLAIR) sequence of MRI as a preoperative diagnosis of hippocampal sclerosis. *No Shinkei Geka* 1998;26(2):143–50 [in Japanese].
20. Mitchell MR, Tarr RW, Conturo TE, et al. Spin echo technique selection: basic principles for choosing MRI pulse sequence timing intervals. *Radiographics* 1986;6(2):245–60.
21. Mitchell MR, Conturo TE, Gruber TJ, et al. AUR Memorial Award. Two computer models for selection of optimal magnetic resonance imaging (MRI) pulse sequence timing. *Invest Radiol* 1984;19(5):350–60.
22. Goddard P, Waring J, Case A, et al. The STIR sequence in MRI of neoplastic lesions. *Bristol Med Chir J (1963)* 1988;103(2):26.
23. Tokuda O, Harada Y, Shiraishi G, et al. MRI of the anatomical structures of the knee: the proton density-weighted fast spin-echo sequence vs the proton density-weighted fast-recovery fast spin-echo sequence. *Br J Radiol* 2012;85(1017):e686–93.
24. Lufkin RB, Keen R, Rhodes M, et al. MRI simulator for instruction in pulse-sequence selection. *AJR Am J Roentgenol* 1986;147(1):199–202.
25. Merboldt KD, Bruhn H, Frahm J, et al. MRI of “diffusion” in the human brain: new results using a modified CE-FAST sequence. *Magn Reson Med* 1989;9(3):423–9.
26. Genovese E, Cani A, Rizzo S, et al. Comparison between MRI with spin-echo echo-planar diffusion-weighted sequence (DWI) and histology in the diagnosis of soft-tissue tumours. *Radiol Med* 2011;116(4):644–56.
27. Idiyatullin D, Corum C, Moeller S, et al. Dental magnetic resonance imaging: making the invisible visible. *J endodontics* 2011;37(6):745–52.
28. Piao R, Iguchi S, Hamada M, et al. High resolution NMR measurements using a 400MHz NMR with an (RE)Ba₂Cu₃O_{7-x} high-temperature superconducting inner coil: towards a compact super-high-field NMR. *J Magn Reson* 2016;263:164–71.
29. Besheer A, Caysa H, Metz H, et al. Benchtop-MRI for in vivo imaging using a macromolecular contrast agent based on hydroxyethyl starch (HES). *Int J Pharm* 2011;417(1–2):196–203.
30. Flugge T, Hovener JB, Ludwig U, et al. Magnetic resonance imaging of intraoral hard and soft tissues using an intraoral coil and FLASH sequences. *Eur Radiol* 2016;26(12):4616–23.
31. Prager M, Heiland S, Gareis D, et al. Dental MRI using a dedicated RF-coil at 3 Tesla. *J Craniomaxillofac Surg* 2015;43(10):2175–82.
32. Sedlacik J, Kutzner D, Khokale A, et al. Optimized 14 + 1 receive coil array and position system for 3D high-resolution MRI of dental and maxillomandibular structures. *Dentomaxillofac Radiol* 2016;45(1):20150177.
33. Idiyatullin D, Corum CA, Nixdorf DR, et al. Intraoral approach for imaging teeth using the transverse B1 field components of an occlusally oriented loop coil. *Magn Reson Med* 2014;72(1):160–5.
34. Ludwig U, Eisenbeiss AK, Scheifele C, et al. Dental MRI using wireless intraoral coils. *Sci Rep* 2016;6:23301.
35. Bracher AK, Hofmann C, Bornstedt A, et al. Feasibility of ultra-short echo time (UTE) magnetic resonance imaging for identification of carious lesions. *Magn Reson Med* 2011;66(2):538–45.
36. Weiger M, Pruessmann KP, Bracher AK, et al. High-resolution ZTE imaging of human teeth. *NMR Biomed* 2012;25(10):1144–51.
37. Idiyatullin D, Garwood M, Gaalaas L, et al. Role of MRI for detecting micro cracks in teeth. *Dentomaxillofac Radiol* 2016;45(7):20160150.

38. Burris NS, Hope MD. 4D flow MRI applications for aortic disease. *Magn Reson Imaging Clin N Am* 2015;23(1):15–23.
39. Liu Y, Gu Y, Yu X. Assessing tissue metabolism by phosphorous-31 magnetic resonance spectroscopy and imaging: a methodology review. *Quant Imaging Med Surg* 2017;7(6):707–26.
40. Arab A, Wojna-Pelczar A, Khairnar A, et al. Principles of diffusion kurtosis imaging and its role in early diagnosis of neurodegenerative disorders. *Brain Res Bull* 2018;139:91–8.
41. Terumitsu M, Matsuzawa H, Seo K, et al. High-contrast high-resolution imaging of posttraumatic mandibular nerve by 3DAC-PROPELLER magnetic resonance imaging: correlation with the severity of sensory disturbance. *Oral Surg Oral Med Oral Pathol Oral Radiol* 2017;124(1):85–94.